

## **Sensitivity-Driven Log-Linear Modelling of Time-to-Peak for Enhanced Flood Forecasting in Heterogeneous Canadian Catchments**

**Vinay Kumar Chukka<sup>1</sup> and Tirupati Boliseti<sup>2</sup>**

Department of Civil and Environmental Engineering, University of Windsor, Windsor, Ontario, Canada<sup>1</sup>

E-mail: [vinaykumarchukka05@gmail.com](mailto:vinaykumarchukka05@gmail.com)

Department of Civil and Environmental Engineering, University of Windsor, Windsor, Ontario, Canada<sup>2</sup>

E-mail: [tirupati@uwindsor.ca](mailto:tirupati@uwindsor.ca)

### **ABSTRACT**

Accurate estimation of the time-to-peak ( $T_p$ ) of a synthetic unit hydrograph (SUH) is essential for flood routing, urban drainage design, and real-time hydrological forecasting. Classical SUH approaches, such as Snyder and Taylor-Schwarz (TS), primarily rely on watershed geomorphology and neglect rainfall variability and catchment-specific heterogeneity. This limitation can lead to large prediction errors under diverse hydrological conditions, particularly in rapidly urbanizing or variable-slope catchments. This study develops and evaluates a data-driven empirical model for  $T_p$  that explicitly integrates catchment characteristics (main channel length ( $L$ ), centroidal length ( $L_c$ ), slope ( $S$ ), roughness ( $n$ ), and imperviousness ( $U$ )) and event-specific inputs (storm duration ( $D$ ) and intensity ( $I$ )). A dataset of 69 rainfall-runoff events from seven Canadian catchments was compiled and analyzed to derive a multi-parameter formulation using least squares nonlinear regression. Model sensitivity was assessed using perturbation and exponent-based elasticity analyses to quantify the influence of geomorphic and rainfall parameters. The proposed model achieved strong predictive capability (Calibration:  $R^2 = 0.745$ ,  $NSE = 0.742$ ; Validation:  $R^2 = 0.876$ ,  $NSE = 0.85$ ) and demonstrated balanced performance for a wide range of catchment scales and land-use conditions. In contrast, Snyder's method showed moderate correlation but poor efficiency ( $R^2 = 0.4$ ,  $NSE = -0.98$ ), while the TS model exhibited extremely weak predictive skill ( $R^2 = 0.024$ ,  $NSE = -24.215$ ), often overestimating  $T_p$  by more than 100-500%. Sensitivity analysis revealed that channel roughness and storm duration exert the strongest influence on  $T_p$ , whereas rainfall intensity has a relatively weak impact. The findings confirm that coupling geomorphic indices with rainfall event properties yields substantially improved  $T_p$  estimation for SUH applications. The proposed model provides a robust tool for flood forecasting and urban drainage planning, particularly in data-rich regions where traditional SUH methods are insufficient. This enhanced responsiveness makes the model directly applicable to real-time flood-forecasting frameworks.

**KEYWORDS:** Synthetic Unit Hydrograph; Time-to-Peak; Parameter Estimation, Log-Linear Optimization, Local One-at-a-Time (OAT) Sensitivity Analysis, Snyder's Time-to-Peak, Flood Forecasting.

## 1 INTRODUCTION

The reliable prediction of hydrological response to rainfall remains fundamental to flood estimation, stormwater design, reservoir operation, and real-time flood forecasting. One of the most enduring methods used for this purpose is the synthetic unit hydrograph (SUH), a conceptual representation of runoff produced by a unit depth of effective rainfall over a watershed. Among its parameters, the time-to-peak ( $T_p$ ) is particularly crucial because it governs peak discharge timing, affects flood routing, and dictates infrastructure design capacity. Despite recent advancements in physically distributed and high-resolution modelling frameworks, SUH remains widely practiced due to its simplicity, low data demand, and adaptability to ungauged conditions (Sarangi et al., 2006). However, classical SUH derivations such as Snyder's method, developed in the 1930s, rely almost entirely on watershed geomorphology and do not account for rainfall dynamics or catchment heterogeneity (Paquet, 2019). This neglect has been questioned in modern hydrology, especially at a time when rapid urbanization and erratic climate-driven precipitation patterns strongly influence watershed response, as discussed by Acanal (2021). Snyder's method assumes that  $T_p$  can be expressed using empirical constants that represent basin shape and response time; however, several studies indicate that regional calibration limits its applicability beyond the region in which its constants were developed. In particular, regions experiencing increased imperviousness, land-use shifts, and nonlinear rainfall intensities tend to show hydrograph responses that diverge significantly from Snyder-based predictions (Bhunya et al., 2007; Chothe & Devappa, 2023). Although the Taylor-Schwarz (TS) model attempted to integrate geomorphology more explicitly into hydrograph prediction, it remained rooted in the assumption that channel networks alone dictate response time, disregarding rainfall variability, infiltration, storage, and storm characteristics. In contemporary studies, the TS model has repeatedly been shown to substantially overpredict  $T_p$ , especially in small, steep, or urban-influenced watersheds, causing errors that can reach several hundred percent (Tunas et al., 2017; Zhu et al., 2025). As climate variability increases short-duration intense storms, hydrologists have emphasized that relying solely on morphometric parameters is increasingly inadequate. A growing body of research supports integrating rainfall intensity, storm duration, and anthropogenic modifications such as imperviousness into empirical hydrograph models to enhance predictive performance (Adib et al., 2019; Ewea et al., 2016). With improvements in rainfall measurement networks, high-resolution geospatial data, and computational analytics, data-driven hydrology has emerged as a bridge between classical empirical approaches and modern physically-based modelling. Unlike purely machine-learning hydrographs, which often lack physical interpretability and are difficult to standardize into engineering practice, hybrid empirical models can combine statistical calibration with mechanistic understanding (Ajami et al., 2016; Singh, 2019). Notwithstanding these advancements, most existing data-driven SUH studies remain limited by small sample sizes, omission of key rainfall variables, weak sensitivity evaluation, or excessive regionalization that restricts broader application (Ghorbani et al., 2019). Moreover, the influence of urban imperviousness and channel roughness, two parameters known to significantly alter runoff concentration time, remains largely underexplored in SUH formulations (Chothe & Devappa, 2023). The absence of these parameters in conventional models leads to systematic biases, particularly for contemporary basins that are no longer purely natural systems. As cities continue to expand and rainfall intensities become more erratic, the need for a transferable, physically interpretable, and data-driven SUH  $T_p$  formulation becomes increasingly evident.

The research presented in this paper aims to fill this research gap by developing a multi-parameter empirical model that integrates both morphometric and rainfall-dependent variables to

estimate  $T_p$ . Based on data collected from seven diverse Canadian watersheds, the model employs nonlinear regression to relate  $T_p$  with the main channel length ( $L$ ), centroidal length ( $L_c$ ), slope ( $S$ ), surface roughness ( $n$ ), fractional imperviousness ( $U$ ), storm duration ( $D$ ), and rainfall intensity ( $I$ ). Unlike classical SUH models that treat hydrographs as physiographic products, this model considers runoff as a dynamic outcome of both landscape structure and storm forcing. The inclusion of dual sensitivity diagnostics, consisting of perturbation-based and elasticity-based analyses, enhances transparency by quantifying relative contributions of each parameter. In order to maintain physical consistency and interpretability of the model, we introduce two sensitivity diagnostics that can assess the effect of each parameter using perturbation-based and elasticity-based approaches. In general, the proposed formulation is conceived to be a physically based and more flexible alternative compared with traditional SUH methods for advancing stormwater design, flood-risk assessment, and infrastructure planning in the face of evolving land-use and climate patterns. Although the primary contribution of this research lies in advancing the empirical estimation of  $T_p$ , the implications extend far beyond hydrograph characterization. Time-to-peak is a foundational predictor for short-term flood forecasting because it governs the lead time available for emergency response, real-time reservoir regulation, and anticipatory operation of stormwater infrastructure. By explicitly incorporating the parameters  $L$ ,  $L_c$ ,  $S$ ,  $n$ ,  $U$ ,  $D$ , and  $I$ , the proposed model produces  $T_p$  estimates that are dynamically responsive to event-scale hydrometeorological forcing.

## 2 TEST CATCHMENTS AND DATA

The analysis was carried out using seven contrasting watersheds across Canada (refer to Figure 1), representing a wide range of hydrogeomorphic and land-use conditions, from predominantly natural basins to highly urbanized systems. Geomorphic attributes were extracted through a GIS-based watershed delineation workflow using high-resolution DEMs, from which drainage boundaries,  $L$ , and  $L_c$  were determined using flow direction and accumulation algorithms.



Figure 1: Location of the seven study catchments.

Slope ( $S$ ) was calculated as an area-weighted average of local slopes derived from the DEM, while  $n$  was assigned using land-cover classifications that translated surface characteristics into Manning’s coefficients. Fractional imperviousness ( $U$ ) was quantified as the ratio of paved and built-up area to total watershed area, obtained from land-use data and validated through high-resolution imagery (see Table 1).

Table 1 Watershed characteristics of the seven Canadian catchments used for  $T_p$  model evaluation.

Catchment	L (Km)	Lc (Km)	S (m/m)	n	U (0-1)
A	22.87	12.48	0.00025	0.13	0.16
B	9.64	4.97	0.00025	0.17	0.31
C	26.58	10.79	0.00083	0.13	0.42
D	6.04	4.22	0.00035	0.10	0.61
E	13.25	12.82	0.00347	0.11	0.39
F	10.68	5.78	0.00290	0.19	0.21
G	16.59	11.09	0.00240	0.25	0.12

The selected watersheds display substantial variability in geomorphic and surface properties. Catchments A and C contain long natural channels; Catchment B has short and steep flow paths;

Catchments D and E exhibit urban drainage influence; Catchment F reflects mixed agricultural and natural characteristics; and Catchment G combines moderate imperviousness with steeper slopes. This diversity in  $L$ ,  $L_c$ ,  $S$ ,  $n$ , and  $U$  provides a robust basis for evaluating  $T_p$  generation under varying runoff conditions. The compiled geospatial database and delineated drainage maps, therefore, supply the necessary physical descriptors to support empirical model development for  $T_p$  estimation.

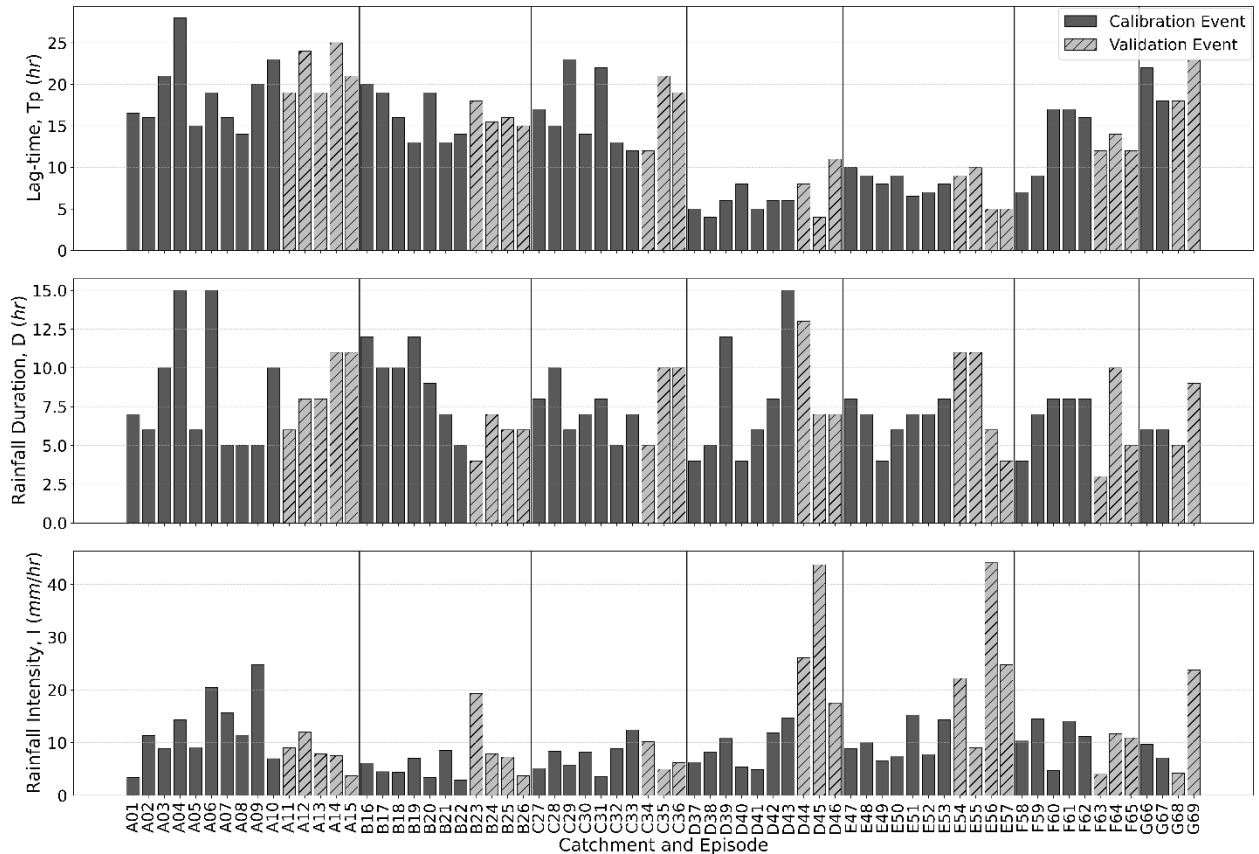


Figure 2: Rainfall-runoff event characteristics ( $T_p$ ,  $D$ ,  $I$ )

A total of 69 rainfall-runoff events were extracted from hydrographs for the seven study watersheds as shown in Figure 2, representing a wide range of storm characteristics from short-duration convective bursts to medium- and long-duration stratiform systems. Rainfall data were obtained from the NASA POWER website, from which mean rainfall intensity ( $I$ ) and storm duration ( $D$ ) were derived after aggregating sub-hourly records to the event scale. To ensure physical consistency, only events exhibiting a single, distinct hydrograph peak were retained, and each event was screened to avoid periods with antecedent or trailing rainfall, thereby isolating runoff response to a single storm without carryover effects. Additional quality checks included exclusion of snowmelt-driven events, verification against backwater or storage impacts, and cross-validation of cumulative rainfall depths with station totals. This rigorous filtering ensured that extracted  $T_p$  values reflect direct rainfall-driven hydrologic response, yielding a reliable dataset for empirical model calibration and sensitivity analysis.

### 3 TRADITIONAL SUH METHODS

#### 3.1 Snyder's Method

Snyder proposed one of the earliest SUH methods, in which the  $T_p$  is estimated using basin geomorphology (Snyder, 1935). The relationship assumes that runoff travel time increases with stream length and basin shape and is calibrated using a regional coefficient  $C_t$  (see Eqs. 1) that reflects watershed characteristics such as slope, storage, and channel configuration. The simplified formulation is:

$$T_p = C_t(LL_c)^{0.3} \quad (1)$$

where  $C_t$  is a nondimensional constant and in general varies from 1.8 to 2.2,  $L$  is the length of the main channel, and  $L_c$  is the distance between the centroid of the catchment and the outlet.

#### 3.2 Taylor and Schwarz (TS) Model

The TS model (Taylor & Schwarz, 1952) is another classical synthetic hydrograph method built on geomorphic controls, but unlike Snyder's formulation, it emphasizes the structure of the drainage network. The method assumes that the basin response time is primarily governed by the channel system and expresses the  $T_p$  as a function of  $L$  and  $S$ , accounting for regional channel geometry. The simplified expression is:

$$S_e = \left[ \frac{N}{\sum_{i=1}^N \left( \frac{1}{S_i} \right)^{0.5}} \right]^2 \quad (2)$$

$$T_p = \left( \frac{0.6}{S_e^{0.5}} \right) e^{(m_1 D)} \quad (3)$$

$$m_1 = 0.212(LL_c)^{-0.36} \quad (4)$$

where  $S_e$  is the average slope of the main channel,  $S_i$  is the slope of the  $i^{th}$  reach of the main channel, and  $N$  is the total number of reaches. In Eqs. (3) - (4),  $T_p$ ,  $L$ , and  $L_c$  are the same as Snyder's method, for  $D$ -hour rainfall in Unit Hydrograph duration.

### 4 PARAMETERS AND DEVELOPMENT OF THE PROPOSED MODEL

#### 4.1 Model Parameters

Parameter selection was guided by the need to represent both the physical structure of the watershed and the variability of individual rainfall events in a hydrologically meaningful way. Four geomorphic descriptors were incorporated as determinants of flow routing and travel time:  $L$ ,  $L_c$ ,  $S$ , and  $n$ . These descriptors together characterize the spatial distribution of the drainage network and

the resistance offered by catchment surfaces, thereby influencing the velocity and timing of runoff concentration. Basin imperviousness ( $U$ ) was introduced as a surface characteristic reflecting the degree of land sealing, which affects infiltration reduction, storage loss, and acceleration of overland flow generation, particularly in urbanizing watersheds.

To represent storm-driven variability, two event-based parameters were included:  $D$  and  $I$ . These rainfall descriptors capture the persistence and volume-loading rate of precipitation, which determine excess rainfall availability and the buildup of runoff over the catchment. The response variable,  $T_p$ , expressed in hours, was manually extracted from observed hydrographs by identifying the elapsed time between the onset of effective rainfall and the peak of direct runoff. To estimate  $T_p$  using combined watershed and storm controls, a nonlinear empirical model was developed as shown in Eqs. (6).

$$T_p = f(L, L_c, S, n, U, D, I) \quad (5)$$

$$T_p = K(LL_c)^\delta S^\alpha n^\beta U^\gamma D^\phi I^\eta \quad (6)$$

Where  $T_p$  is lag-time ( $hr$ ),  $L$  is main channel length ( $km$ ),  $L_c$  is centroidal channel length ( $km$ ),  $S$  is basin slope,  $n$  is Manning's roughness coefficient (-),  $U$  is fractional imperviousness (0-1),  $D$  is rainfall duration ( $hr$ ),  $I$  is mean rainfall intensity ( $mm/hr$ ) and  $(K, \delta, \alpha, \beta, \gamma, \phi, \eta)$  are empirical coefficients or exponents.

The combined use of geomorphic, land-surface, and rainfall characteristics allows for a physically interpretable representation of watershed response while maintaining sensitivity to event-specific forcing. Collectively, these eight variables provide a robust foundation for developing a transferable empirical formulation for  $T_p$  that can account for hydrologic variability across diverse catchment types and storm conditions.

## 4.2 Model Development

The empirical model for estimating  $T_p$  was formulated using a nonlinear multiplicative structure to preserve hydrologic interpretability and reflect the scaling behaviour inherent in watershed response. A power-law representation was selected to relate  $T_p$  to geomorphic attributes, land-surface characteristics, and storm controls as shown in Eqs. (6). The formulation consists of a dimensionless constant and elasticity-type exponents associated with model parameters

presented in subchapter 4.1. The nonlinear least-squares optimization was conducted, minimizing squared deviations between observed and simulated  $T_p$  while retaining physically meaningful exponent signs to avoid unrealistic influences on routing time.

To avoid model overfitting and evaluate predictive transferability, the dataset of 69 rainfall-runoff events was split into calibration (70%) and validation (30%) subsets for each catchment (as shown in Figure 2). The first subset was used to optimize the empirical coefficients, and the resulting calibrated model was then applied to the remaining events without further adjustment. Predictive skill was assessed through the coefficient of determination ( $R^2$ ) and Nash–Sutcliffe Efficiency (NSE), ensuring that both correlation strength and magnitude-based agreement were quantified.

To examine the influence of individual predictors and validate the physical plausibility of calibrated exponents, a Local one-at-a-time (OAT) sensitivity assessment was performed. Perturbation diagnostics quantified the change in  $T_p$  under  $\pm 10\%$  variations in each input, while log-elasticity inspection exploited the exponent structure of the power-law form to interpret proportional response sensitivities. Together, these diagnostics provided a consistent sensitivity hierarchy and confirmed that the calibrated model responds to contour length, roughness, storm duration, and imperviousness in agreement with expected hydrological behaviour.

## 5 RESULTS AND DISCUSSION

After nonlinear optimization, the regression procedure yielded the calibrated coefficients for both catchment-scale and rainfall-driven parameters, which are presented in Eqs. (7).

$$T_p = 7.16(LL_c)^{0.311}S^{-0.169}n^{1.205}U^{0.04}D^{0.246}I^{-0.08} \quad (7)$$

### 5.1 Performance of Proposed Model

The proposed empirical formulation demonstrated strong predictive capability across both calibration and validation datasets. During calibration, the model achieved  $R^2 = 0.745$  and  $NSE = 0.742$ , indicating that the simulated  $T_p$  closely reproduced the observed temporal patterns without structural bias. Validation confirmed even higher skill, yielding  $R^2 = 0.876$  and  $NSE = 0.85$ , showing that the optimized coefficients generalized well to independent events without recalibration, as shown in Figure 3.

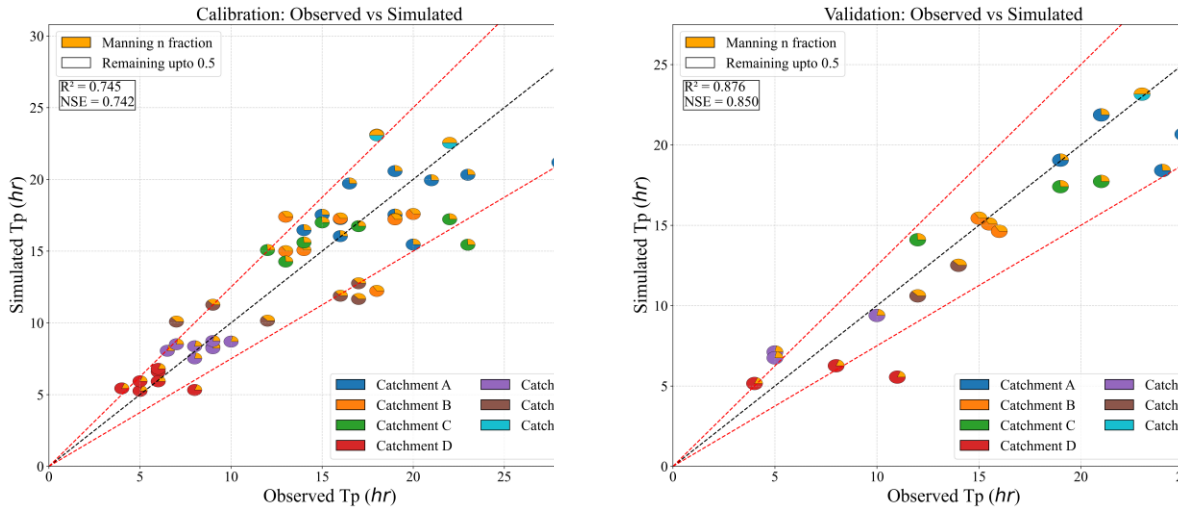


Figure 3: Observed vs simulated  $T_p$  for calibration and validation datasets.

Observed versus modeled scatter plots clustered tightly around the 1:1 line, and a majority of points fell within the  $\pm 25\%$  acceptance bounds, demonstrating stability across a wide range of watershed sizes and storm conditions. Error statistics further support the robustness of the proposed formulation. In calibration, the percent error ranged between 0.28% and 44.13%, with a mean absolute error of  $\approx 17.2\%$ .

Validation showed even smaller deviations, which ranged from 0.29% up to 49.52%, with a lower average of about 14.4% (refer to Figure 3). The largest discrepancies were concentrated in small, rapid-response systems (e.g., Catchment D), where even minute uncertainties in rainfall onset, sensor latency, or temporal aggregation disproportionately distort hydrograph rise and peak timing. Runoff translation in these basins is dominated by super-concentrated travel times, low levels of surface storage and channel attenuation, resulting in an abrupt change to the  $T_p$  with relatively small changes to storm duration or intensity. Consequently, the model's continuous empirical scaling, although robust for moderate and large basins, becomes more sensitive in these highly reactive hydrologic regimes, where  $T_p$  exhibits threshold-like behavior rather than gradual scaling. In these rapid-response systems, model bias remained lower than benchmark methods, highlighting improved temporal accuracy in routing estimation.

## 5.2 Comparison with Standard Models

For benchmarking, the proposed formulation was compared against Snyder's and the TS model,

both of which rely solely on geomorphologic scaling and omit rainfall and land-surface variability. Each model was executed using the same input dataset, allowing differences in performance to be attributed solely to structural modelling assumptions rather than data inconsistency. Evaluation metrics included  $R^2$ , NSE, and relative  $T_p$  prediction error, thus quantifying both bias and statistical fidelity.

To evaluate the limits of the Snyder method, a “Land-Use Adapted” approach was also tested, wherein the  $C_i$  coefficient was step-wise reduced from 2.0 to 1.1 based on catchment imperviousness. Despite this adaptive parameterization intended to capture urban flow acceleration, the method yielded an NSE of -0.98, confirming that coefficient calibration alone cannot compensate for the omission of rainfall dynamics. Benchmark comparisons against Snyder’s and TS models showed substantial performance limitations in classical SUH formulations. Snyder’s method produced  $R^2 = 0.4$ , whereas the TS model performed even worse, with  $R^2 = 0.024$  and  $NSE = -24.21$ . These negative NSE values indicate that both traditional models predict  $T_p$  less accurately than the mean of observed values, signifying strong systematic bias. Snyder’s approach is primarily based on watershed geometry, which results in approximately the invariant  $T_p$  predictions; the points are projected onto a single line (see Figure 4). On the other hand, the TS method is considered more dynamic as well as diverse rainfall and consequently shows an even greater scatter with higher deviation when different rainfall inputs are used for different events.

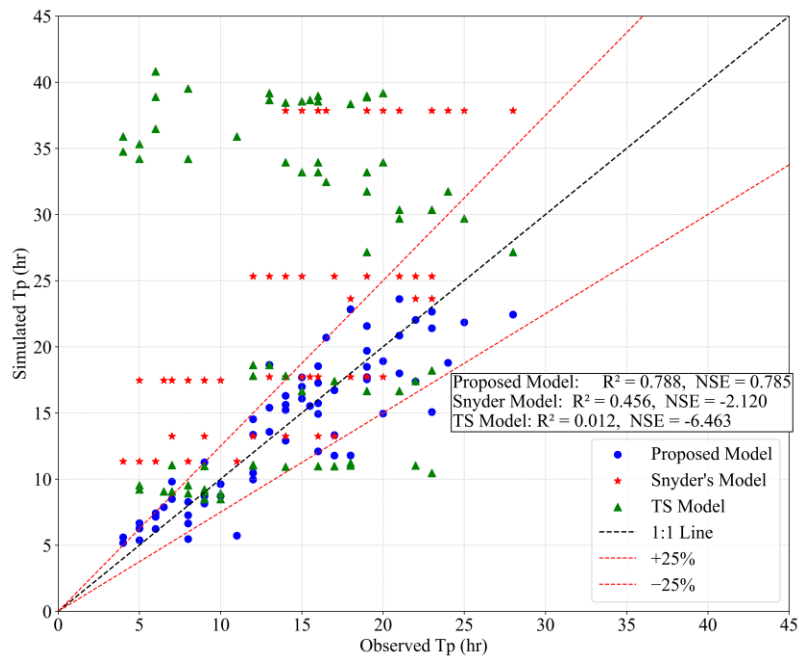


Figure 4: Performance comparison of the proposed  $T_p$  model with standard prediction models against observations.

Across all catchments, Snyder’s and TS formulations consistently overestimated  $T_p$  values, frequently by **100-500%**, particularly in highly impervious or fast-draining basins. For example, Catchment D (urbanized channelized basin), which has observed  $T_p$  values of 4-11 hours, was predicted to be 11-40 hours by benchmark models. This overestimation stems from an exclusive reliance on geomorphology-based scaling, without accounting for the rapid storm-runoff acceleration caused by urban surfaces, rainfall duration, or direct channel roughness effects. The results clearly indicate that traditional SUH methods are insufficient for contemporary stormwater-dominated landscapes where precipitation dynamics and land-use alterations significantly alter hydrograph response.

### 5.3 Sensitivity Analysis Findings

Sensitivity diagnostics indicate that  $T_p$  is controlled predominantly by  $n$ , with  $D$  and  $L$  exerting secondary influence, whereas  $U$ ,  $S$ , and  $I$  display comparatively minor effects. The primacy of  $n$  reflects its role in hydraulic retardation and momentum dissipation, elongating travel time even under small perturbations, while  $D$  governs temporal runoff accumulation, aligning peak timing with rainfall persistence rather than intensity. Incremental increases in  $U$  accelerate hydrograph response by reducing infiltration losses, whereas the weak sensitivity of  $I$  confirms that peak timing is a routing-dominated process rather than an intensity-driven phenomenon.

Accordingly, calibration and validation scatterplots were rendered with pie-fractional markers (0-0.5 range) to explicitly encode the spatial variability of  $n$  (see Figure 3), emphasizing its disproportionate leverage in controlling hydrograph timing. These findings affirm that urban flood timing is governed primarily by frictional impedance and storm persistence, highlighting the inadequacy of classical SUH models that ignore these controls and consequently distort peak discharge estimation in stormwater design (refer to Figure 5).

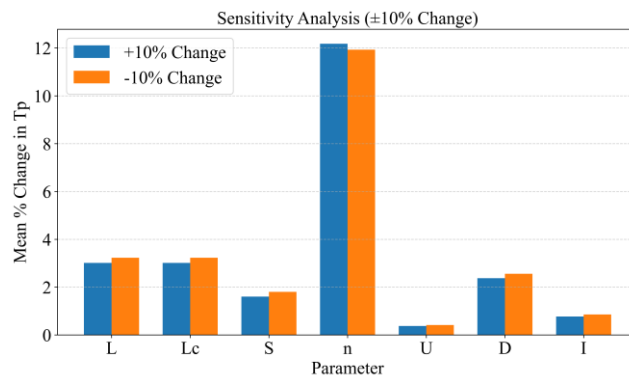


Figure 5: Sensitivity of  $T_p$  to  $\pm 10\%$  perturbations in model parameters.

## 5.4 Application of the Proposed Model to Flood Forecasting

The proposed  $T_p$  formulation provides immediate value for flood-forecasting systems by enabling rapid, event-responsive estimation of hydrograph timing. Unlike traditional SUH parameters that assume static watershed behavior, the model incorporates rainfall persistence,  $U$ , and  $n$ , allowing  $T_p$  predictions to adjust dynamically to evolving storm characteristics. Its elasticity-based structure enables forecasters to infer how changes in  $D$  or watershed conditions will shift  $T_p$ , supporting proactive reservoir operation and urban drainage management.

Because the model captures travel-time compression in highly impervious or fast-responding basins, it delivers more realistic  $T_p$  than classical SUH methods, especially during short, intense events. When coupled with radar rainfall or ensemble precipitation forecasts, it can generate continuously updated  $T_p$  estimates suitable for real-time decision-support tools and early-warning platforms. Thus, beyond enhancing SUH parameterization, the model functions as a computationally efficient component for operational flood forecasting in rapidly changing and urbanized watersheds.

## 6 CONCLUSIONS

This investigation demonstrates that  $T_p$  estimation in Canadian watersheds cannot be credibly represented using traditional geomorpho-centric SUH formulations that disregard rainfall controls and land-surface heterogeneity. The proposed nonlinear, multi-parameter  $T_p$  model, calibrated across seven hydroclimatically contrasting basins, substantially outperforms canonical approaches (e.g., Snyder; TS), which exhibited systematic bias and overprediction stemming from their exclusion of storm persistence and imperviousness. The newly derived exponent structure and sensitivity hierarchy reveal that routing resistance, particularly manifest through  $n$ , is the paramount regulator of hydrograph temporal translation, while  $D$  and  $L$  impose secondary constraints, thereby confirming that fluvial impedance and rainfall temporal load supersede instantaneous rainfall rate in peak-timing control. By integrating geomorphic resistance, storm structure, and anthropogenic surface alteration into a single transferable formulation, this model delivers a physically interpretable and computationally efficient tool adaptable to evolving Canadian hydroscares under urbanization and climatic intensification. Consequently, the model enables superior prediction of hydrograph lag, reduces structural underdesign risks, and provides a defensible basis for flood-routing design, low-impact drainage planning, and real-time peak-flow forecasting within a broad spectrum of Canadian watershed typologies. By providing a dynamically responsive and computationally lightweight formulation for  $T_p$ , the model is readily deployable within early-warning systems, real-time hydrograph generation modules, and event-based flood-forecasting platforms where accurate  $T_p$  prediction is indispensable.

## REFERENCES

- Acanal, N. (2021). Snyder-gamma synthetic unit hydrograph. *Arabian Journal of Geosciences*, 14(4), 271-. <https://doi.org/10.1007/S12517-021-06531-7>

- Adib, A., Lotfirad, M., & Haghghi, A. (2019). Using uncertainty and sensitivity analysis for finding the best rainfall-runoff model in mountainous watersheds (Case study: the Navrood watershed in Iran). *Journal of Mountain Science*, 16(3), 529–541. <https://doi.org/10.1007/S11629-018-5010-6>
- Ajami, H., Khan, U., Tuteja, N. K., & Sharma, A. (2016). Development of a computationally efficient semi-distributed hydrologic modeling application for soil moisture, lateral flow and runoff simulation. *Environmental Modelling & Software*, 85, 319–331. <https://doi.org/10.1016/J.ENVSOFT.2016.09.002>
- Bhunya, P. K., Berndtsson, R., Ojha, C. S. P., & Mishra, S. K. (2007). Suitability of Gamma, Chi-square, Weibull, and Beta distributions as synthetic unit hydrographs. *Journal of Hydrology*, 334(1–2), 28–38. <https://doi.org/10.1016/J.JHYDROL.2006.09.022>
- Chothe, O. K., & Devappa, V. (2023). Synthetic unit hydrograph for ungauged basin using Snyder, Taylor- Schwarz model, SCS method by GIS techniques. *Materials Today: Proceedings*, 77, 855–859. <https://doi.org/10.1016/J.MATPR.2022.11.505>
- Ewea, H. A., Elfeki, A. M. M., Bahrawi, J. A., & Al-Amri, N. S. (2016). Sensitivity analysis of runoff hydrographs due to temporal rainfall patterns in Makkah Al-Mukkramah region, Saudi Arabia. *Arabian Journal of Geosciences*, 9(5), 424-. <https://doi.org/10.1007/S12517-016-2443-5>
- Gede Tunas, I., Anwar, N., & Lasminto, U. (2017). Parameters Estimation of Synthetic Unit Hydrograph Model Using Multiple Linear and Non-linear Regressions. *2nd International Conference on Applied Mathematics*.
- Ghorbani, K., Salarijazi, M., Abdolhosseini, M., Eslamian, S., & Ahmadianfar, I. (2019). Evaluation of Clark IUH in rainfall-runoff modelling (case study: Amameh Basin). *International Journal of Hydrology Science and Technology*, 9(2), 137–153. <https://doi.org/10.1504/IJHST.2019.098131>
- Paquet, E. (2019). Synthetic hydrograph generation by hydrological donors. *Hydrological Sciences Journal*, 64(5), 570–586. <https://doi.org/10.1080/02626667.2019.1593418>
- Sarangi, A., Madramootoo, C. A., Enright, P., & Prasher, S. O. (2006). Evaluation of three unit hydrograph models to predict the surface runoff from a Canadian watershed. *Water Resources Management*, 21(7), 1127–1143. <https://doi.org/10.1007/S11269-006-9072-9>
- Singh, S. K. (2019). Dynamic parameter estimation for hydrological model. *International Journal of Hydrology Science and Technology*, 9(2), 124–136. <https://doi.org/10.1504/IJHST.2019.098159>
- Snyder, F. F. (1935). Synthetic Unit Hydrograph. *Trans Am Geophysical Union*, 19, 447–454.
- Taylor, A. B., & Schwarz, H. E. (1952). Unit hydrograph lag and peak flow related to basin characteristics. *Trans Am Geophys Union*, 33, 235–246.
- Zhu, W., Ianculescu, D., & Anghel, C. G. (2025). Synthetic Hydrograph Estimation for Ungauged Basins: Exploring the Role of Statistical Distributions. *Stats*, 8(4), 100. <https://doi.org/10.3390/STATS8040100>

Websites:

Web-1: <https://power.larc.nasa.gov/>

Web-1: [https://wateroffice.ec.gc.ca/mainmenu/real\\_time\\_data\\_index\\_e.html](https://wateroffice.ec.gc.ca/mainmenu/real_time_data_index_e.html)